

# Spinodal Decomposition in Polymer Mixtures via Surface Diffusion

J. Klein Wolterink<sup>1</sup>, G.T. Barkema<sup>1</sup> and Sanjay Puri<sup>2</sup>

<sup>1</sup> *Institute for Theoretical Physics, Utrecht University,  
Leuvenlaan 4, 3584 CE Utrecht, THE NETHERLANDS.*

<sup>2</sup> *School of Physical Sciences, Jawaharlal Nehru University, New Delhi – 110067, INDIA.*

## Abstract

We present experimental results for spinodal decomposition in polymer mixtures of gelatin and dextran. The domain growth law is found to be consistent with  $t^{1/4}$ -growth over extended time-regimes. Similar results are obtained from lattice simulations of a polymer mixture. This slow growth arises due to the suppression of the bulk mobility of polymers. In that case, spinodal decomposition is driven by the diffusive transport of material along domain interfaces, which gives rise to a  $t^{1/4}$ -growth law.

PACS numbers:

A homogeneous binary mixture (AB) becomes thermodynamically unstable when it is quenched into the miscibility gap. The subsequent evolution of the mixture is characterized by the emergence and growth of domains enriched in either component [1, 2, 3]. This process of *domain growth* or *coarsening* or *spinodal decomposition* is of great technological and scientific importance, and is relevant in diverse applications, e.g., the food-processing industry, metallurgy, materials science, structure formation in the early universe, etc. The standard experimental tools to characterize domain growth are (a) the time-dependence of the typical domain size  $\ell(t)$ ; and (b) the functional form of the structure factor, which depends on the system morphology. The domain growth law depends critically on the mechanism which drives phase separation. For example, diffusive transport of material through bulk domains yields the Lifshitz-Slyozov (LS) growth law  $\ell(t) \sim t^{1/3}$ , whereas diffusion along surfaces (interfaces) gives rise to a slower growth law  $\ell(t) \sim t^{1/4}$  [4, 5, 6, 7]. For binary fluid mixtures, the intermediate and late stages of phase separation are driven by the advective transport of material. The relevant growth laws (in  $d = 3$ ) are  $\ell(t) \sim t$  in the *viscous hydrodynamic* regime, followed by  $\ell(t) \sim t^{2/3}$  in the *inertial hydrodynamic* regime [1, 2, 3].

In the food-processing industry, many applications involve domain growth in demixing polymer blends or quasi-binary polymer solutions (i.e., two kinds of polymers in a solvent). Polymeric phase separation has been studied experimentally in films of polymer blends [8, 9, 10, 11], in thicker samples [12, 13], and in soluted mixtures [14]. The typical time-scales of decomposition in these experiments vary from seconds [14] to days [13]. To characterize the speed of the coarsening process, one often fits a power-law to the location  $q_{\max}$  of the maximum in the structure factor, as a function of time. Measurements of the resulting growth exponent  $\alpha$  in  $q_{\max} \sim t^{-\alpha}$  range from 0 to 0.45 [8, 10, 11]. Wilzius and Cumming [12] report a value of  $\alpha \simeq 0.28$ ; Kuwahara et al [13] report an evolution of this exponent from  $\alpha \simeq 0$  to  $\alpha \simeq 0.3$ ; and Takeno and Hashimoto [9] measure a value between 0.25 and 0.33. Clearly, there is no consensus on the experimental side regarding the growth law. Moreover, the dominant mechanism for domain growth may differ in various experiments and time-regimes, explaining the diverse exponents reported in the literature.

In this letter, we present results from an experimental and numerical study of spinodal decomposition in polymer mixtures in the high-viscosity regime (i.e., without hydrodynamics). First, we will present results from a light-scattering study of phase separation in a

mixture of gelatin and dextran, soluted in water. For deep quenches, domain growth in this system is consistent with the growth law  $\ell(t) \sim t^{1/4}$ . Next, we will present numerical results obtained from a lattice simulation of spinodal decomposition in a polymer mixture. Again, the domain growth law is found to be compatible with  $\ell(t) \sim t^{1/4}$  over an extended time-regime. We interpret these growth laws in the context of phase separation driven by surface diffusion, as the bulk mobility is drastically reduced in these polymer mixtures due to a large free-energy barrier for releasing a component from its concentrated phase. We conclude this letter with a discussion of the growth exponent which characterizes surface diffusion, and the crossover from surface to bulk diffusion.

Let us first present details of the experiments. The chemicals used for the spinodal decomposition experiments were gelatin (fish gelatin with a high molecular weight, Multi Products, Lot 9187, box 47) and dextran (obtained from Sigma, industrial grade with an average molecular weight of 181 kg/mol, D-4876, Lot 41K1243). These chemicals were used without further purification. The concentration in the final sample for gelatin was 2.46% and for dextran 2.40% w/w. No salt was added to the solution. However, azide was added to the stock solutions to halt bacterial growth. The light-scattering set-up used is shown in Fig. 2 of Tromp et al [15]. A He/Ne laser (633 nm) was used to generate a scattering pattern that was projected onto a screen of tracing paper. This is recorded by a CCD-camera (EG & G PARC, Model 1430P). (See also Lundell et al [16].) The usable  $q$ -range was  $0.3\text{-}7 \mu\text{m}^{-1}$ .

The gelatin-dextran mixture described above is homogeneous at room temperature and starts to demix at a temperature of  $\simeq 8^\circ\text{C}$ . The phase separation is clearly visible at  $6^\circ\text{C}$ . This is close to the gelation temperature of the gelatin, which is estimated as  $8\text{-}10^\circ\text{C}$  [17]. We specifically selected this mixture to obtain a high viscosity, so that hydrodynamic effects can be ignored on the time-scales of our experiments.

Starting with a homogeneous mixture, we performed either a shallow quench to a final temperature of  $5^\circ\text{C}$ , or a deep quench to  $1^\circ\text{C}$ . From then on, the structure of the coarsening mixture is recorded at regular times with light scattering. Specifically, we obtain the typical domain size from  $\ell(t) = 2\pi/q_{\text{max}}(t)$ , where  $q_{\text{max}}(t)$  is the location where the spherically-averaged structure factor  $S(q, t)$  reaches its maximum. Due to practical reasons, the time  $t_0$  of the onset of phase separation is not known precisely in our experiments. We therefore determine  $t_0$  from our measurements of  $S(q, t)$  as follows. Assuming that the domain growth process is described by  $q_{\text{max}}(t) \sim (t - t_0)^{-\alpha}$  with  $\alpha \simeq 1/4$  or  $1/3$ , we perform a linear least-

squares fit in which  $q_{\max}^{-1/\alpha}$  is plotted vs.  $t$ ; the time of zero-crossing is then our estimate of  $t_0$ . Since it takes some time before the structure factor develops a clear peak, we repeated this procedure also for the locations  $q'_{\max}$  and  $q''_{\max}$  of the maxima in  $qS(q, t)$  and  $q^2S(q, t)$ . This results in six estimates for  $t_0$ , which we average. We use the average value of  $t_0$  to make a double-logarithmic plot of  $\ell(t)$  vs.  $(t - t_0)$ ; the result is shown in Fig. 1.

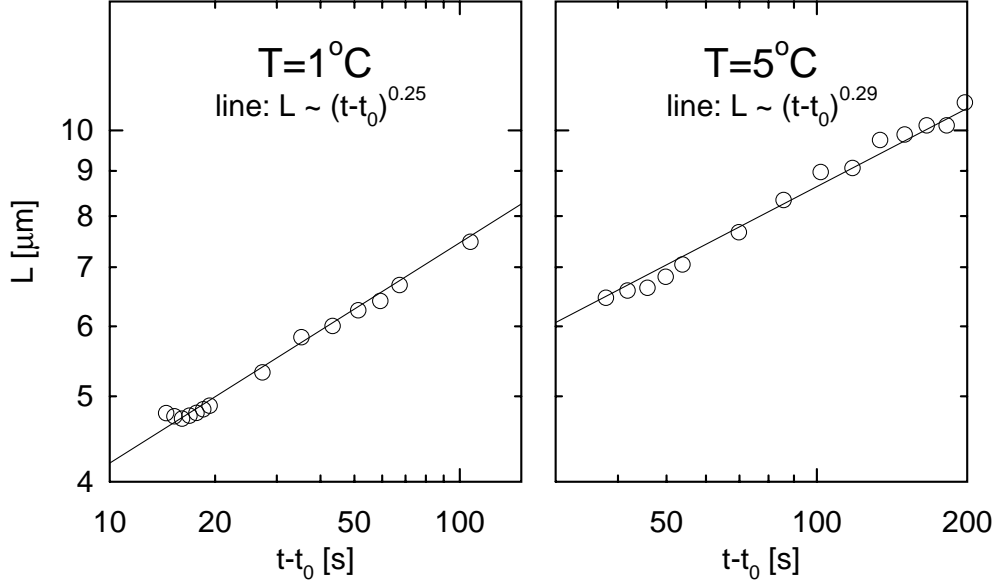


FIG. 1: Time-dependence of length scale from experiments, plotted on a log-log scale. We study a deep quench to  $1^\circ\text{C}$  (left frame) and a shallow quench to  $5^\circ\text{C}$  (right frame). The lines denote the best linear fits to the experimental data. The corresponding growth exponents are specified in the figure.

As the straight lines in the figure indicate, domain growth after a deep quench to  $1^\circ\text{C}$  is fitted well by  $\ell(t) \sim (t - t_0)^{0.25}$ , and after a shallow quench to  $5^\circ\text{C}$  by  $\ell(t) \sim (t - t_0)^{0.29}$ . The deep quench shows convincingly a domain growth exponent in agreement with surface diffusion. The shallow-quench experiment is not so conclusive. The larger growth exponent indicates that both surface and bulk diffusion contribute to coarsening, and we are in a crossover regime between  $\alpha = 1/4$  and  $\alpha = 1/3$ . As we will discuss shortly, the bulk mobility is enhanced at higher temperatures where A-rich bulk domains contain significant amounts of B, and vice versa.

We have also performed extensive simulations of spinodal decomposition in a quasi-binary polymer mixture. The specific model that we used is a lattice polymer model. Polymers with

$N$  bonds are described in this model as self-avoiding and mutually-avoiding walks on a face-centered-cubic (FCC) lattice. The polymers move by a sequence of single-monomer jumps to nearest-neighbor lattice sites. For monomers which are neighbors along the same polymer, the steric interactions are lifted (and a site can thus be occupied by two or more adjacent monomers), as this allows enhanced reptation. Both reptation and Rouse dynamics are captured qualitatively in this model. Therefore, it can be used to study dynamical properties with some degree of realism, as long as hydrodynamic interactions are not essential. The model is described in detail by Heukelum and Barkema [18]. It has previously been used to study the fractionation of polydispersed polymer mixtures [19], diffusion and exchange of adsorbed polymers [20], and desorption of polymers [21].

The current study involves 128,000 polymers, each consisting of  $N = 50$  bonds and connecting 51 monomers. These are located on a 3-dimensional FCC lattice with  $8 \times 10^6$  sites and periodic boundary conditions. Half of the polymers are labeled as type A, and the other half as type B. Polymers of different type repel each other: the total energy is equal to the number of pairs of neighboring sites occupied by different-type polymers, multiplied by an energy scale  $J$ . If an attempted Monte Carlo (MC) move increases the total energy by  $\Delta E$ , the acceptance probability of this move is  $P_a = \exp(-\beta\Delta E)$ , where  $\beta = 1/(k_B T)$  is the inverse temperature. Moves which do not raise the total energy are always accepted.

The simulations start from a mixed state, generated as an equilibrium configuration at high temperature ( $\beta = 0$ ). At  $t = 0$ , the temperature is quenched to either  $\beta J = 0.05$  or  $\beta J = 0.1$ . At these low temperatures, the repulsive AB interactions induce phase separation into domains rich in either A or B. The size of these domains grows in time – evolution snapshots for a typical run are shown in Fig. 2. To characterize domain growth, we assign to lattice site  $i$  occupied by an A-type (B-type) polymer the value  $\sigma_i = +1$  ( $\sigma_i = -1$ ). The domain size is defined as the distance  $\ell$  of the first zero-crossing of the spatial correlation function of  $\sigma_i$ , and we measure it at various times. The time-dependence of  $\ell(t)$  is shown in Fig. 3. After an initial transient regime, both data sets (for  $\beta J = 0.05, 0.1$ ) are consistent with the growth law  $\ell(t) \sim t^{1/4}$  over extended time-regimes, viz.,  $\sim 2$  decades for  $\beta J = 0.05$  (denoted by circles), and  $\sim 2.5$  decades for  $\beta J = 0.1$  (denoted by squares).

The above experimental and numerical results can be understood in the following theoretical framework. The kinetics of phase separation is described by the Cahn-Hilliard (CH)

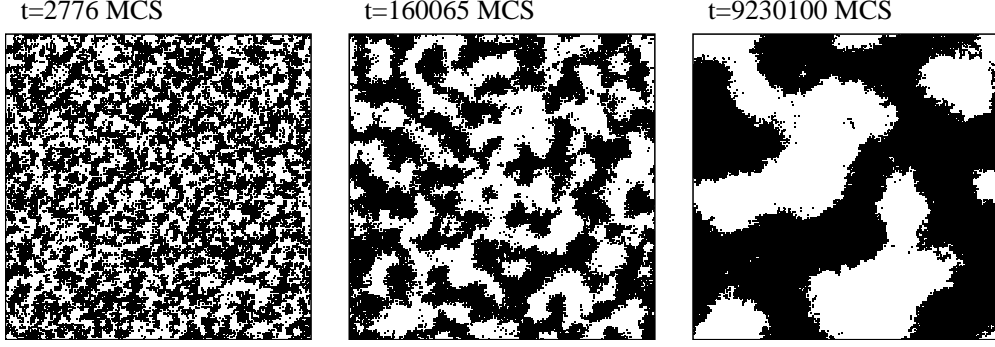


FIG. 2: Evolution pictures from simulations of spinodal decomposition in polymer mixtures. Details of the simulation are described in the text. The quench temperature was  $\beta J = 0.1$ , and the system size is  $200^3$ . The species A is marked in black, and the species B is not marked. The time in Monte Carlo steps (MCS) is indicated above each snapshot.

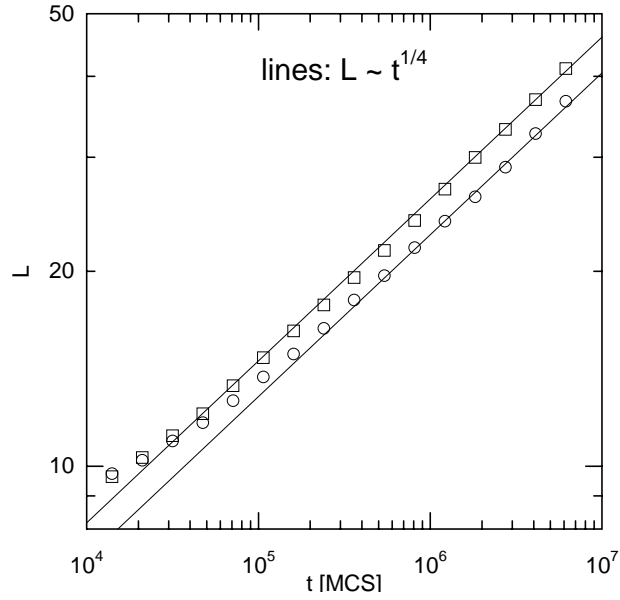


FIG. 3: Time-dependence of length scale from simulations, plotted on a log-log scale. The time is measured in MCS. We show data for quenches to  $\beta J = 0.05$  (circles), and  $\beta J = 0.1$  (squares). The lines correspond to the growth law  $\ell(t) \sim t^{1/4}$ .

model [1, 2, 3]:

$$\frac{\partial}{\partial t} \psi(\vec{r}, t) = \vec{\nabla} \cdot \left[ D(\psi) \vec{\nabla} \left( \frac{\delta F}{\delta \psi} \right) \right], \quad (1)$$

where  $\psi(\vec{r}, t)$  is the order parameter at space point  $\vec{r}$  and time  $t$ . Typically,  $\psi(\vec{r}, t) \simeq \rho_A(\vec{r}, t) - \rho_B(\vec{r}, t)$ , where  $\rho_A$  and  $\rho_B$  denote the local densities of species A and B. We have neglected thermal fluctuations in Eq. (1), and considered the general case of a  $\psi$ -dependent

mobility  $D(\psi)$  [22, 23, 24]. Further,  $F[\psi]$  denotes the Helmholtz potential, which is usually taken to have the  $\psi^4$ -form:  $F[\psi] \simeq \int d\vec{r} \left[ -\psi^2/2 + \psi^4/4 + (\vec{\nabla}\psi)^2/2 \right]$ , where we have used the order-parameter scale and the bulk correlation length to express  $F[\psi]$  in dimensionless units.

Let us consider a situation where the mobility at the interfaces ( $\psi = 0$ ) is  $D_s$ , and that in the bulk ( $\psi = \pm 1$ ) is  $D_b$ , with  $D_b \leq D_s$ . This difference in interfacial and bulk mobilities can result from low-temperature dynamics, where there is a high energy barrier for an A-atom to enter a B-rich bulk domain and vice versa. Alternatively, physical processes like glass formation [25] or gelation [26, 27] can also result in a drastic reduction in bulk mobility. A simple functional form for the mobility in the above case is  $D(\psi) = D_s(1 - \alpha\psi^2)$ ,  $\alpha = 1 - D_b/D_s$ . Notice that  $0 \leq \alpha \leq 1$  for  $D_b \leq D_s$ . Thus, Eq. (1) can be written as

$$\frac{\partial}{\partial t}\psi(\vec{r}, t) = \vec{\nabla} \cdot \left[ (1 - \alpha\psi^2) \vec{\nabla} (-\psi + \psi^3 - \nabla^2\psi) \right], \quad (2)$$

where we have absorbed  $D_s$  into the time-scale.

Equation (2) can be decomposed as [5]

$$\frac{\partial}{\partial t}\psi(\vec{r}, t) = (1 - \alpha)\nabla^2(-\psi + \psi^3 - \nabla^2\psi) + \alpha\vec{\nabla} \cdot \left[ (1 - \psi^2) \vec{\nabla} (-\psi + \psi^3 - \nabla^2\psi) \right], \quad (3)$$

where the first term on the RHS corresponds to bulk diffusion. This term is absent in the limit  $\alpha = 1$  ( $D_b = 0$ ). The second term on the RHS corresponds to surface diffusion. It is only relevant at interfaces, where  $\psi \simeq 0$ . The location of the interfaces  $\vec{r}_i(t)$  is defined by the zeros of the order-parameter field,  $\psi[\vec{r}_i(t), t] = 0$ . Let us focus on a particular interface in the  $d$ -dimensional case. We denote the normal coordinate as  $n$  and the interfacial coordinates as  $\vec{a}$  [with dimensionality  $(d - 1)$ ]. Then, the normal velocity  $v_n(\vec{a}, t)$  obeys the integro-differential equation [4, 5]:

$$4 \int d\vec{a}' G[\vec{r}_i(\vec{a}), \vec{r}_i(\vec{a}')] v_n(\vec{a}', t) \simeq (1 - \alpha)\sigma K(\vec{a}, t) + 4\alpha \int d\vec{a}' G[\vec{r}_i(\vec{a}), \vec{r}_i(\vec{a}')] \nabla^2 K(\vec{a}', t). \quad (4)$$

Here,  $K(\vec{a}, t)$  is the local curvature at point  $\vec{a}$  on the interface, and  $\sigma$  is the surface tension. The Green's function  $G(\vec{x}, \vec{x}')$  is obtained from  $-\nabla^2 G(\vec{x}, \vec{x}') = \delta(\vec{x} - \vec{x}')$ .

A dimensional analysis of Eq. (4) yields the growth laws due to surface and bulk diffusion. We identify the scales of various quantities in Eq. (4) as

$$\begin{aligned} [d\vec{a}] &\sim \ell^{d-1}, & [G] &\sim \ell^{2-d}, \\ [v_n] &\sim \frac{d\ell}{dt}, & [K] &\sim \ell^{-1}. \end{aligned} \quad (5)$$

This yields the crossover behavior of the length scale as

$$\begin{aligned}\ell(t) &\sim (\alpha t)^{1/4}, \quad t \ll t_c, \\ &\sim [(1 - \alpha)\sigma t]^{1/3}, \quad t \gg t_c,\end{aligned}\tag{6}$$

where  $t_c \sim \alpha^3/[(1 - \alpha)^4\sigma^4]$ . Notice that the asymptotic regime obeys the LS growth law, which is characteristic of growth driven by bulk diffusion. However, the crossover to the LS regime can be strongly delayed if the bulk mobility is suppressed relative to the surface mobility, i.e.,  $D_b/D_s \rightarrow 0$  or  $\alpha \rightarrow 1$ .

In conclusion, we have presented results from both experiments and simulations of spinodal decomposition in polymer mixtures. In both cases, we find an extended time-regime where the domain growth law is compatible with  $\ell(t) \sim t^{1/4}$ . This slower growth law arises because there is a strong suppression of mobility in bulk domains due to a large energy barrier to dissolve in the polymer-poor phase. Therefore, domain growth is primarily driven by diffusive transport along interfacial regions, which gives rise to a  $t^{1/4}$ -growth law. Understanding the mechanism of demixing is not only important for identifying the domain growth exponent, it is also a pre-requisite for obtaining control over the structure formation. We hope that the results presented here will stimulate further experimental and numerical interest in this fascinating problem.

Acknowledgment: We would like to thank Hans Tromp from NIZO food research for his kind hospitality, and Arjan Visser for preliminary simulations.

- 
- [1] A.J. Bray, *Adv. Phys.* **43**, 357 (1994).
  - [2] K. Binder and P. Fratzl, in *Phase Transformations in Materials*, edited by G. Kostorz (Wiley-VCH, Weinheim, 2001), p. 409.
  - [3] A. Onuki, *Phase Transition Dynamics* (Cambridge University Press, Cambridge, 2002).
  - [4] T. Ohta, *J. Phys. C* **21**, L361 (1988); K. Kawasaki and T. Ohta, *Prog. Theor. Phys.* **68**, 129 (1982).
  - [5] A.M. Lacasta, A. Hernandez-Machado, J.M. Sancho and R. Toral, *Phys. Rev. B* **45**, 5276 (1992); A.M. Lacasta, J.M. Sancho, A. Hernandez-Machado and R. Toral, *Phys. Rev. B* **48**, 6854 (1993).



- [6] S. Puri, A.J. Bray and J.L. Lebowitz, Phys. Rev. E **56**, 758 (1997).
- [7] S. van Gemmert, G.T. Barkema and S. Puri, Phys. Rev. E **72**, 046131 (2005).
- [8] J. Lauger, R. Lay and W. Gronski, J. Chem. Phys. **101**, 7181 (1994).
- [9] H. Takeno and T. Hashimoto, J. Chem. Phys. **108**, 1225 (1998).
- [10] M. Hayashi, H. Jinnai and T. Hashimoto, J. Chem. Phys. **113**, 7554 (2000).
- [11] M. Hayashi, H. Jinnai and T. Hashimoto, J. Chem. Phys. **112**, 6886, 6897 (2000).
- [12] P. Wiltzius and A. Cumming, Phys. Rev. Lett. **66**, 3000 (1991).
- [13] N. Kuwahara, H. Sato and K. Kubota, J. Chem. Phys. **97**, 5905 (1992).
- [14] B. Steinhoff, M. Rullmann, L. Kuhne and I. Alig, J. Chem. Phys. **107**, 5217 (1997).
- [15] R. H. Tromp, A. R. Rennie and R. A. L. Jones, Macromolecules **28**, 4129 (1995).
- [16] C. Lundell, E. H. A. de Hoog, R. H. Tromp and A. M. Hermansson, J. Colloids Interface Sci. **288**, 222 (2005).
- [17] R. H. Tromp, E. ten Grotenhuis and C. Olieman, Food Hydrocoll. **16**, 235 (2002).
- [18] A. van Heukelum and G. T. Barkema, J. Chem. Phys. **119**, 8197 (2003).
- [19] A. van Heukelum, G. T. Barkema, M. W. Edelman, E. van der Linden, E. H. A. de Hoog and R. H. Tromp, Macromolecules **36**, 6662 (2003).
- [20] J. Klein Wolterink, G.T. Barkema and M.A. Cohen Stuart, Macromolecules **38**, 2009 (2005).
- [21] J. Klein Wolterink, M.A. Cohen Stuart and G.T. Barkema, Mol. Phys. (in press).
- [22] J.S. Langer, M. Bar-on and H.D. Miller, Phys. Rev. A **11**, 1417 (1975).
- [23] K. Kitahara and M. Imada, Prog. Theor. Phys. Suppl. **64**, 65 (1978); K. Kitahara, Y. Oono and D. Jasnow, Mod. Phys. Lett. B **2**, 765 (1988).
- [24] S. Puri, K. Binder and S. Dattagupta, Phys. Rev. B **46**, 98 (1992); S. Puri, N. Parekh and S. Dattagupta, J. Stat. Phys. **77**, 839 (1994).
- [25] D. Sappelt and J. Jackle, Europhys. Lett. **37**, 13 (1997); Polymer **39**, 5253 (1998).
- [26] F. Sciortino, R. Bansil, H.E. Stanley and P. Alstrom, Phys. Rev. E **47**, 4615 (1993).
- [27] J. Sharma and S. Puri, Phys. Rev. E **64**, 021513 (2001).